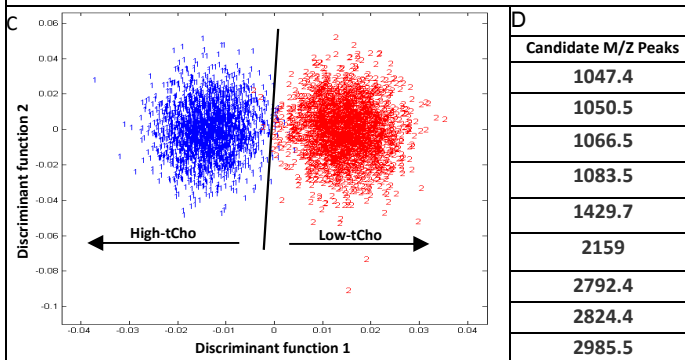
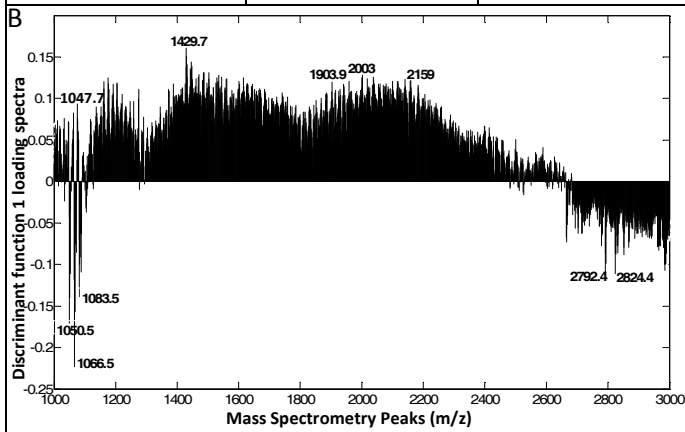
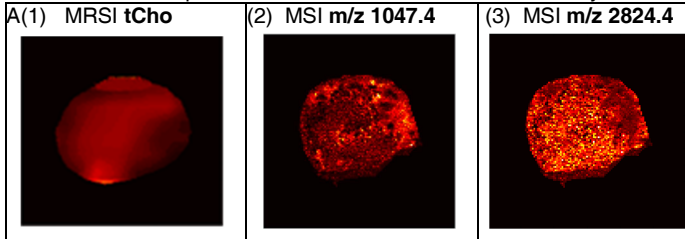


Combining MRSI and Mass Spectrometric Imaging Reveals Protein Biomarkers in Breast Tumor Models

Lu Jiang¹, Kamila Chughtai², Tiffany Greenwood¹, Gert Eijkel², Ron Heeren², and Kristine Glunde¹

¹Division of Cancer Imaging Research, Department of Radiotherapy, Johns Hopkins School of Medicine, BALTIMORE, MD, United States, ²FOM-Institute AMOLF, Amsterdam, Netherlands

Introduction: The intensity of the total choline (tCho) signal in magnetic resonance spectroscopic imaging (MRSI) of tumors is spatially heterogeneous. Magnetic resonance spectroscopy (MRS) studies have shown an elevation of phosphocholine (PCho) and total choline-containing metabolites (tCho) in breast cancer cells and tumors [1]. Our previous study [2] investigated the relationship between tCho and membrane phosphatidylcholine (PC) species which can be detected by mass spectrometric imaging (MSI) of histologic tumor sections. In this study, we have further investigated the correlations between tCho and proteins in a human breast cancer model by combining *in vivo* magnetic resonance imaging (MRI) and MRSI with *ex vivo* MSI.



Candidate M/z Peaks
1047.4
1050.5
1066.5
1083.5
1429.7
2159
2792.4
2824.4
2985.5

Figure A (1): MRSI tCho map (3.2 ppm) of breast tumor xenograft; and corresponding MALDI MSI map of m/z 1047.4 (Figure A (2)) and m/z 2792.4 (Figure A (3)). B: Discriminant function 1 loading spectra of 4999 randomly selected high-tCho-containing and low-tCho-containing voxels. C: Scattering plot of discriminant function 1 and function 2 scores obtained in the classification of high- and low-tCho-containing voxels. D: Candidate MALDI MSI peaks obtained by our data analysis.

Methods: Human MDA-MB-231-HRE-tdTomato breast cancer cells were orthotopically grown in nude mice. Both 3-dimensional (3D) water-suppressed H¹ MRSI to detect water, and water-suppressed 3D MRSI to detect metabolites, was performed on tumors *in vivo*. Inherently registered 3D T1-weighted images were acquired to measure the tumor anatomic structure as a reference for MRSI. Each tumor was cryo-sectioned into fiducially marked 10- μ m thick slices to perform MSI. On-tissue tryptic digest followed by matrix-assisted laser desorption ionization (MALDI) MSI was performed on a Q-TOF instrument (Synapt, Waters) as described previously [2, 3] to detect peptides that were generated by the tryptic digest from larger proteins. We used our co-registration platform based on Ponceau S fiducial markers and shape characteristics that allowed us to fuse MRI, MRSI, MSI images [4]. The 3D tCho volume was segmented by considering the voxels above 10% of the area under the histogram as high-tCho-containing area. The remaining voxels under 10% were considered as the low-tCho-containing area. The corresponding 3D MALDI high-tCho-containing and 3D MALDI low-tCho-containing voxels were pooled, from which 2499 high-tCho-containing voxels and 2500 low-tCho-containing voxels were selected randomly, followed by principal component analysis (PCA) to reduce the dimension and noise of these MALDI MSI data. 95% variance of the PCA projection data was analyzed by Fisher linear discriminant analysis (FDA) to classify high-tCho-containing voxels and low-tCho-containing voxels through these MALDI data. The m/z range between m/z 1000 and m/z 3000 of MALDI MSI data was analyzed and the loading spectra of discriminant function 1 were sorted to select candidate m/z peaks, which mostly contributed to the differentiation between high- and low-tCho-containing voxels. The molecular m/z peak candidates were identified by searching a peptide database with the resulting m/z values as keywords. **Results:** tCho (3.2 ppm) was observed by *in vivo* MRSI (Fig. A (1)). Several peptides from hypoxia up-regulated protein 1 (HYOU1, m/z 1047.4) as well as peptides from ribosomal proteins such as m/z 1066.5, m/z 1429.7 and 2824.4 displayed the highest peaks in the discriminant function 1 loading spectrum obtained from MALDI MSI data. Fig. A (1) shows a representative MRSI tCho map. Fig. A (2) and (3) show the corresponding MALDI MSI distribution of HYOU1 (m/z 1047.4) and ribosomal protein (m/z 2824.4). Fig. B shows the discriminant function 1 loading spectrum of 4999 randomly selected high- and low-tCho labeled voxels in MALDI MSI. Fig. C shows the scattering plot of FDA discriminant function 1 and function 2 scores obtained in the classification of high-tCho-containing and low-tCho-containing voxels. Fig. D lists candidate molecular m/z peaks of tryptic peptides obtained by our classification analysis. **Discussion and Conclusions:** In our previous study [4], tCho was increased in the hypoxic regions of breast tumor xenografts. However, the HYOU1 peak at m/z 1047.4 was negatively correlated with the corresponding tCho signal in MRSI data. HYOU1 is up-regulated by hypoxia [5] and is associated with poor prognosis in breast cancer [6]. The relative decrease of HYOU1 protein in regions of high tCho is currently undergoing further investigation in our lab. The molecular ions at m/z 1066.5, 1429.7 and 2824.4 were identified as ribosomal proteins that positively correlated with the tCho map in MRSI. This finding suggests that increased biosynthesis of ribosomal proteins may happen in high tCho regions in breast tumors. All other identified tryptic peptides are

currently undergoing further validation by ion fragmentation studies using MSI-based MS/MS methods. By combining MRSI with tryptic on-tissue digest and MALDI MSI, followed by registration and data analysis based on tCho-voxel classification, PCA, and FDA, we identified for the first time some of the specific proteins that are differentially expressed in breast tumor regions that contain high tCho. **References:** [1]. Glunde et al. (2011), NMR Biomed 24(6):673-90; [2]. Jiang et al. (2012), Abstract #: 178, ISMRM, Melbourne, Australia; [3]. Chughtai et al. (2012), Anal Chem, 84(4):1817-23. [4]. Jiang et al. (2012), Neoplasia 14(8):732-41. [5] Tamatani et al. (2001), Nature Medicine 7:317-323; [6] Stojadinovic et al. (2007), Med Sci Monit 13, BR231-239.

Acknowledgements: This work was supported by NIH R01 CA134695.